Design, simulation and experimental validation of a multiport electrical converter for Standalone Building-Integrated Photovoltaic systems

Víctor Hernández Sierra

Supervisors: Fabrice Frébel and Benoît Bidaine

Faculty of Applied Sciences - University of Liège

Academic Year 2018-2019

Erratum

- An Appendix F, entitled 'Experimental Validation' is added. It is entirely included in this document.
- List of small corrections:

Page	Paragraph	Line	Old Version	Corrected Version
3	5	5	... not attached to...	... not integrated to ...
5	5	7	... with deisregard of...	... with disregard for ...
6	6	2	... control scheme arises ...	... control schemes arises ...
6	7	2	... Differents paths ...	... Different paths ...
11	2	1	... is repsented by ...	... is represented by ...
11	2	2	... or receive the ...	... or receive the ...
15	Figure 3.2		... graphs.	... graphs [23].
16	Eq 3.15 - 3.18		Vo	V3
25	Eq 4.7 - 4.8		Vo	V3
29	1	1	... and current at ...	... and currents at...
34	2	4	... as 1-2 is ...	... as 1-3 is ...
36	5	6	... phase shifted vary ...	... phase shift vary ...
49	6	4	... as following:	... the following:
59	2	6	... as it ...	... to where it ...

Appendix F

Experimental Validation

The experimental validation final phase has been divided into two parts. First, a two-port test has been performed, to assess how the converter behaves under a single conversion stage strategy. Afterwards, a full three-port test has been done, analyzing in detail if ZVS conditions are met.

The two-port test has been performed under operating point C. In this mode, port 1 (PV panels) are fully meeting the load on port 3 (Distribution side) without the intervention of port 2 (Battery). Load has been established at 110 Ω and the port has been fed with a lab power supply. Phase shift has been set at 55 degree for both 1-2 and 1-3, in a similar level as the simulations performed. Figure F.1 depicts the result of one of the tests performed under the mentioned criteria. The red and blue graphs have been taken at one of the outputs of a half-bridge of ports 1 and 3, respectively, related to ground. The brown constant signal depicts the voltage at the load terminals, that is, at port 3.

While the input (red signal) is rated at 25 V, the output signal is risen up to 100 V (note that probes are attenuated by a factor of 1/10 and 1/100 respectively). An efficiency level of 89% has been reached, with an input current of 4.10 A which establishes a 102 W power input. It can be observed that the switching spikes have been attenuated with the introduction of the snubber circuit. However, the resistance factor of the snubber also produces a slow decrease in the square voltage, producing a non-perfect square shape. Losses are therefore present on this snubber circuit solution, as was to be expected. A simulation has been performed to compare the obtained values, and a satisfactory comparison has been established. In simulation, power level is slightly higher (around 130 W), as was to be expected due to losses in experimental testing. However the same behaviour is observed and therefore the 2-port test can be validated.

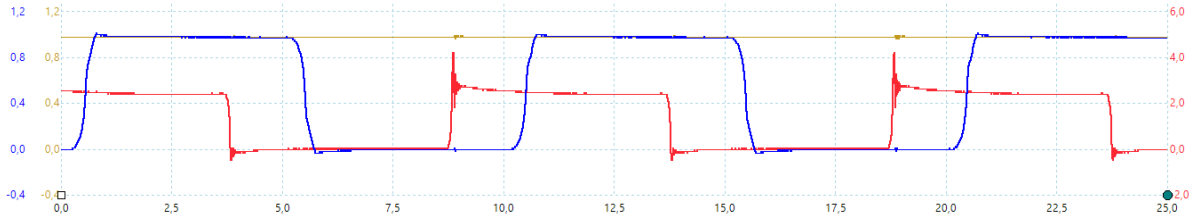

Figure F.1: Square voltage of PV port (red), Battery (blue) and DC output (brown).

Next, a three-port test was to be done. The chosen operating point was B, in which both PV and Battery ports are feeding the distribution side at equilibrium. The resulting signals can be observed in Figure F.2, in which load has been maintained at 110 Ω and phase shift is set at 25 degree for ports 1-3 and 0 for ports 1-2. The red and blue graph represent, respectively, the output square signal of ports 1 and 2 of one of its half-bridges. They are set with a constant input of 29 V and 22.5 V, with a current of 3.88 A and 5.14 A each. This would represent that port 1 is feeding 113 W while port 2 is feeding 115 W, being therefore at the expected equilibrium. The output voltage at the load terminals of port 3, shown in the brown graph, is of 154 V, representing 215 W. Efficiency is therefore of 95%, superior from the 2-port test case.

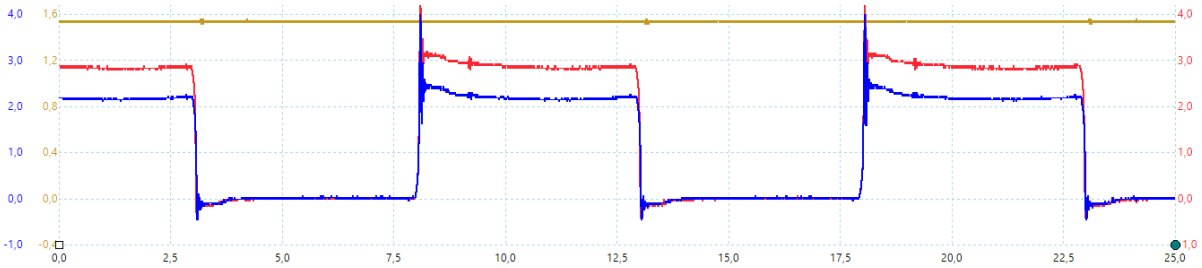

Figure F.2: Square voltage of PV port (red), Battery (blue) and DC output (brown).

Figure F.3 represents the square voltage of port 1 (red graph) and the resonant tank current flowing through the same port (blue graph). Current is lagging its applied voltage, which, as has been studied during the simulation phase, is a sign that the port is working under ZVS conditions. While port 2, the other feeding port, also follows the same trend and is therefore working with lossless transition, port 3 does not meet the require criteria, and losses are occurring during switching.

This phenomena could be due to two different factors. First, as a snubber circuit has been introduced, a difference in circuit behaviour could be induced. This would need to be solved by improving the decoupling method as not to affect the signal variability. The small decrease on the square voltage could also be avoided and efficiency would be further improved. A second explanation could be related to the fact that tests have not been performed under the rated conditions but rather at low load. As was observed during the voltage range analysis, the circuit is designed to operate losslessly if the rated voltages and loads are respected. Further analysis would be required to study how lossless transition could be kept under operation modes that differ from the designed ones.

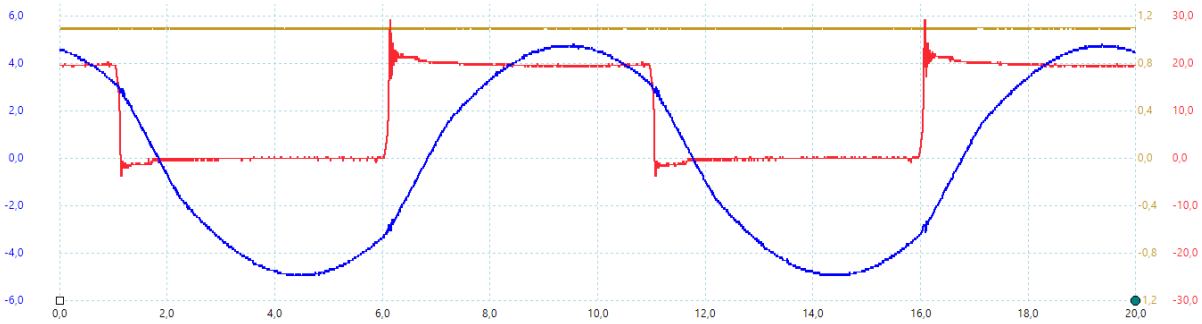

Figure F.3: Square voltage (red) and resonant tank current (blue) at PV port.